Design and optimization of tapered optical fiber probes for SERS utilizing FDTD method

Ciyong Gu
Nanjing University of Aeronautics and Astronautics
Delong Meng
Nanjing University of Aeronautics and Astronautics
Zhimin Zhao
Nanjing University of Aeronautics and Astronautics
Xiaolei Yu (nuxiaolei_yu@163.com)
Nanjing University of Aeronautics and Astronautics https://orcid.org/0000-0003-3134-9734

Research Article

Keywords: Tapered optical fiber, Ag NPs, FDTD simulation, Surface enhanced Raman scattering

Posted Date: May 4th, 2022

DOI: https://doi.org/10.21203/rs.3.rs-1524686/v1

Abstract

In this work, we report a strategy of Ag nanoparticles (Ag NPs) coated tapered optical fiber probes by finite difference time domain (FDTD) simulations. Investigation shows that the fiber tip decorated Ag NPs have excellent electric field enhancement and confinement of light capabilities compared with fiber tips. Moreover, we demonstrate the effect of key parameters such as tip radius, conical angle, Ag NPs size and gaps between them on the field enhanced utilizing typical excitation wavelength of 532, 633 and 785 nm. To further improve the electrical field effect, a noble metal substrate is introduced below the tip apex which exhibits a higher field enhancement generated by tip-substrate coupling. The presence of the Au substrate does not lead to a significant change in the plasma characteristic peak of the probes at 490 nm. This study provides a useful reference for the fabrication of tapered optical fiber with plasmonic nanostructures and the design of robust tapered fiber-optic Raman sensors.

1. Introduction

Sensitive optical fiber as a powerful sensing technology can be used in various applications, such as food safety, environmental, chemical, and biological sensing [1–3]. With the development of optical fiber technology, several studies combining the surface enhanced Raman scattering (SERS) with optical fiber to develop promising LSPR and SERS fiber probe have been reported [4, 5]. Compared with tradition SERS substrates, the fiber probes can not only realize large SERS enhancement but also provide an ideal platform for remote measurements and making in situ sensing possible [6–8]. As a result, the development of excellent SERS-based sensors has received widely attention in both industry and academia.

The key principle of the SERS fiber probes is the preparation of nano-structures at the end of the excitation fiber and modified SERS-active sensing layer such as noble metal nanoparticles and metal films. In addition, it is known fact that the detection sensitivity of the probes is related to the local electric field enhancement generated by the plasma micro/nanostructure, in which the fiber probe can be delivered both the excitation light to the sample and the backscattered SERS signal to the Raman spectrometer. To date, there are various types of optical fiber structures serving developed as SERS fiber probe [9–13]. Although many fibers probe have been prepared and the excellent Raman signals obtained, the practical applications of SERS are still limited especially the knowledge of electromagnetic field enhancement mechanism [14, 15]. The current theoretical analysis method for SERS fiber probes, numerical analysis is a powerful tool for analyzing of electromagnetic field enhancement and for system design of the probes. To obtain high Raman enhancement, several performance improvement methods are usually combined with numerical simulations to optimize the geometry of the fiber probes and shearing the SERS-active layer. Tang et al. [16] successfully have fabricated spherical SERS fiber probes and coated the spherically fiber tips with Ag NPs. The high SERS enhancement factor can be obtained by optimizing the diameter of the fiber spheres. A grid nanostructured SERS fiber sensor using the numerical simulation analysis has presented and shown a double characteristic peak, which offers the possibility to realize plasmon resonance excitation mode [17]. In addition, the field enhancement properties and

parameter optimization of tapered fiber SERS probes coated with Au NPs on their tip have also investigated using the FDTD method [18]. The FDTD method are also applicable to the design of gas fiber probes to analysis of the electric field distribution and polarization properties, and the interpretation of the physical mechanisms [19, 20]. The three-dimensional computation numerical can be used to pinpoint the location of hot spots on the probe surface and to analyze the ultrashort pulse propagation of the tapered optical fiber probe [21]. Both the above theoretical and experimental studies show that the higher SERS sensitivity of the probe are strongly influenced by fiber geometry, and the NPs. At present, various methods are used to fabricate SERS fiber probes with randomly undefined shapes and sizes [22, 23]. This is mainly due to the effect of fiber size, poor operability, and controllability of the fabrication procedures. Therefore, it is necessary to combine numerical modeling simulation to design probes, which can get further insights into the general importance of identified relationships, and reduce production cost and improve production efficiency of the probes. Among them, tapered fiber probes have a larger specific surface area than other shape probe and show many advantages of the high light transmission efficiency and large interaction area for the excitation light and SERS signal [24].

In this study, a FDTD simulations is used to design and to numerical simulate the tapered fiber probes. The results show that the field enhancement properties of the fiber tip modified Ag NPs are significantly improved. Moreover, the relevant parameters including tip radius, cone angles, Ag NPs size and gaps between them were optimized. Finally, the electric field strength can be further improved by introducing a noble metal substrate below the fiber tip. This study provides a realistic theoretical reference for the application study of tapered fiber probes in Raman spectroscopy.

2. Propose Structure Description And Fdtd Simulation

Firstly, we designed a tapered fiber probe with Ag NPs modified on the surface of fiber tip. A default design parameter with a reasonable range of the tapered angle (θ = 41.2°), tip radius (50 nm), Ag NPs radius (50 nm), the gap between Ag NPs (5 nm), and gap between the Ag NPs and fiber tip surface of 1 nm was provided [25]. Subsequently, the full-field electromagnetic simulations were performed using FDTD method via a commercial software package (Lumerical Solutions, Inc.) to investigate the local electric field enhancement and SERS enhancement factor (EF). The base solver directly solves Maxwell's equations in both time and space on a spatial grid where is without any simplifying approximations, making analysis far accurate. Moreover, the FDTD provides three-dimensional (3D) and two-dimensional (2D) models, as well as intuitive CAD modeling windows which is suitable for simulating of any complex model and showing results. To improve simulation efficiency, trade-off memory requirements and simulation time for an ordinary computer, a 2D simulations model of tapered fiber coated with Ag NPs were designed on x-y plane, as shown in Fig. 1. This appropriate simplified 2D scattering problem will not reduce results accuracy [26]. Gaussian Beam was used as excitation light with a same total width as the excitation boundary, and the excitation field amplitude (E_0) was set 1 V/m. The vector K was defined to propagate in the y direction with a polarization mode either in the x- or z-directions (p- and s polarization, respectively). Perfectly matched layers (PML) were used in the x-y directions as the boundaries conditions

to truncate computational regions. According to Drude model, the dielectric constant (ε_m) of Au in the visible and near-IR can be written as [27].

$$\epsilon_m(\omega) = \epsilon_\infty - \frac{\omega_p^2}{\omega^2 + i\omega\omega_c}$$

Where$\epsilon_\infty$is the angular frequency of incident light, ω_p is the plasma frequency of Ag which is the frequency of the oscillations of electron density in the metal, ω_c stands for collision frequency, which corresponds to the damping of electron density oscillations due to collisions among the electrons, and the data are given by Johnson and Christy [28]. As for calculation capability, the mesh spacing is fixed at dx = 0.001 μm and dy = 0.001 μm to ensure accuracy sufficient and stability for this study.

3. Results And Discussion

3.1. Uncoated tapered optical fiber

Before studying other parameters, the optical propagation characteristic in an uncoated tapered optical fiber was analyzed by two different polarization directions. The incident light is perpendicular to excitation boundary, the shape of the fiber tip was determined by tip radius 50 nm, excitation boundary of the radius width 0.8 μm and cone angle of 41.2°. Figure 2 shows the spatial field distribution of the fiber tip calculated by 2D-FDTD simulations. For two different polarizations: Fig. 2(a) is p-polarised and Fig. 2(b) is s-polarised light excited by 785 nm, respectively. The color map represents the maximum electric field value. From this Figure, it can also be observed that the intensity radiation shows an enhancement close to the fiber tip, the electric field intensity ($|E|/|E_0|_{max}$) of a p- and s-polarised is 1.52 and 1.89, respectively. In addition, the tapered region is smaller along the axial direction of the fiber tip and the fiber's cross section decreases due to the tapering of the fiber, resulting the diffractive effect is significantly enhanced and the light escapes to the surrounding area via the evanescent field. The energy of the evanescent field is inherently related to the refractive index, indicating that higher the refractive index of the surrounding medium the fiber, the less confined will be the light in the fiber [25]. Therefore, the uncoated tapered optical fiber is poor confinement of light field in a small cross-section area.

3.2. Tapered optical fiber with Ag nanoparticles

A tapered optical fiber of the local electric field enhancement is investigated when Ag NPs are coated at the fiber tip. As above, the shape of the fiber tip was determined using default value, the radius of the Ag NPs is taken as 50 nm and the gap between them is 5 nm, and the NPs are 1 nm away from the fiber tip surface. For p-polarisation, Fig. 3 shows a simulated electric field distribution of a tapered optical fiber with different wavelengths of 532, 633, and 785 nm. These results demonstrate that the electric field can be significant enhanced in p-polarised light due to the light leaking out from fiber and excitation of localized surface plasmons (LSPs) between the Ag NPs. Furthermore, the "hot spot" which is dependent on the interaction between the nano-structures and excitation light occurs between the Ag NPs, and the

positions moved at different wavelength. The $|E|/|E_0|_{max}$ is arrived at 15.8 in case of tapered optical fiber at 532 nm. For s-polarised light, Fig. 4 shows that the evanescent field uncoupling the LSPs between neighboring Ag NPs, obviously, they do provide a reflective layer, like a mirror, that reflects light back into the tip, creating a standing wave [25]. The maximum electric field intensity is 4.46. The s-polarized electric field characteristics do not exhibit obvious variers in all wavelengths. Thus, we will focus on p-polarized light in the subsequent analyses.

Further, the optical characteristic of the proposed probes was performed which transmission spectrums is measured by frequency-domain field and power, and the monitor present on 20 nm underneath the fiber tip. Figure 5 (a), a peaks concave at 490 nm is observed. This phenomenon indicates that excitation wavelength at 490 nm is due to absorption between the Ag NPs, resulting the transmission spectrum is concaved. For SERS fiber probes, it is important to select the appropriate lasers to excite plasmon which is advantageous in Raman applications and enhanced signals. So, we analyze maximum electric field along a line connecting the Ag NPs at different wavelength, as shown in Fig. 5(b). The result suggests that the electric field intensity in 490 nm is significantly higher than over the whole wavelength from 450 to 800 nm. This is expected since the fiber tip coated Ag NPs, the dip of the transmission spectrum is the signature of the excitation of the fundamental gap plasmon resonance [25, 29]. On the other hand, the p-polarized light with the electric field perpendicular to the tapered surface of the Ag NPs is coupled to the surface Plasmons Polaritons (SPPs) supported TM mode in the probes [30].

3.3 Parameter optimization of tapered optical fiber

Notably, SERS study indicates that optimization geometric parameters of the fiber probes are important, since the optimal fiber probes can obtain most efficient SERS signal and electric field enhancement. Therefore, we simulated four different parameters setting, including tip radius, conical angle, Ag NPs size and the gap between them to record the effect of electric field using most common laser excitation wavelengths of 532, 633 and 785 nm. A single-valued variable method is used for optimization, other parameters set as default tapered angle ($\theta = 41.2°$), tip radius (50 nm), Ag NPs radius (50 nm), the gap between Ag NPs (5 nm), and the gap between an Ag NPs and fiber tip surface is 1 nm. As shown in Fig. 6(a), the effect of tip radius ranges from 50 to 500 nm, the $|E|/|E_0|_{max}$ between Ag NPs along a line connecting the Ag NPs is calculated. Note that the electric field under wavelength of 532 nm is larger than that of 633 and 785nm, especially, when the tip radius is less than 300 nm. As the tip radius is reduced, more evanescent field outside the walls of the taper increases to couple with the NPs and the energy density in the optical fiber increases, resulting the electric field between Ag NPs is also higher. In general, the effect of electric field is stronger in 532 nm and the emission energy is higher compared to the long wavelength. Figure 6(b), the effect of cone angle with varied from 10 to 70° are calculated. The electric field enhancement fluctuated in excitation wavelengths of 532 nm and 633 nm are change more obvious than 785 nm, and the optimum field enhancement is obtained at a cone angle between 25° and 35°, whereas the change of the electric field at excitation wavelength of 785 nm is not significantly in all conical angle. The effect of gap between the Ag NPs on the electric field enhancement curve is investigated, as shown in Fig. 6(c). Figure indeed shows that the electric field intensity is rapidly reduction

as the spacing between the Ag NPs increased. In other words, the strongest hotspots exists when the dimers of Ag NPs gap distance are less 5 nm region, and the enhanced Raman scattering more apparently [31]. Finally, the effect of the Ag NPs radius was evaluated in size range from 30 nm to 100 nm, as shown in Fig. 6(d). As expected, the acquired electric fields at the three wavelengths show that the optimal electric fields at each wavelength corresponds to different NPs size. For 532, 633 and 785 nm excitation, the optimal size of the radius is 55, 70 and 95 nm, respectively. It can be explained that the wavelengths of LSPs are slightly different for certain dimensions of the Ag NPs excitation. Moreover, we observe a redshift of the plasmon resonance wavelength when the NPs radius is increased.

3.4 The tapered optical fiber probe with substrate

In the above analysis, we discuss the field enhancement characteristics of the proposed probes only included fiber tip coated Ag NPs. To further improve the electrical field enhancement, we designed a noble metal (Au) substrate located L = 23 nm below the probes-tip and 2 nm from the Ag NPs, as shown in Fig. 7(a). The higher enhanced electric fields can be found between the tip-substrate coupling and gap region between the Ag NPs in Fig. 7(b). The coupling field enhancement mainly depends on the excitation wavelength, substrate and relative distance between the fiber tip and substrate. Here, we main pay attention to the excitation wavelength is 785 nm. As shown in Fig. 7(c), the field intensity of the tip-substrate coupling is significantly larger than the fiber tip without substrate with a wavelength range between 450 to 800 nm. At the same time, the two curves have the same change in electric field strength at the maximum peak of 490 nm, and we note that the presence of the Au substrate does not lead to a significant change in the wavelength at 490 nm. This again proves that the peak of 490nm is represent plasmon resonance peak generated between Ag NPs on the fiber tip surface, because the wavelength of plasmon resonance peak of the fiber probes is not related to the substrate. Figure 7(d) shows the variation of the electric field in the x-y plane with the gap between the fiber tip-substrate, which the gap distance was defined as L varied from 23 to 400 nm. It is show that the strong electric field is reduced as the increase of distance L, when the L is less than 26 nm the maximum electric field arrived at 22.3 attributed by tip-substrate coupling. Whereas, when the distance L was greater than 26 nm, the electric field between adjacent Ag NPs is higher than tip-substrate coupling mainly dominated by both plasmonic gap-modes and image-force effect [32]. On the other hand, As the distance increased the field strength between silver nanoparticles is enhanced, which can effectively avoid the detection distance problem in the application of probe detection. Further, Fig. 8 is investigated the effective model area in both model that is the tip without substrate coupling Fig. 8(a) and the tip-substrate coupling Fig. 8(b). The latter has a higher enhancement of the electric field and the effective mode area severely reduced due to strong mode coupling.

Finally, we compared the fields enhancement that two substrate-Au and Ag were used to evaluate the tip-substrate coupling efficiency. The structural parameters of the probe are consistent with above. Table 1 shows that field enhancement performance is best for the Ag substrate, followed by Au, which is calculated by numerical simulation. In addition, the EF were calculated that the probes with Ag substrates have stronger EF in wavelengths of 532nm. On the contrary, Au substrates have a more stable EF in

different wavelength. In the actual SERS system, the Ag substrate obviously has a larger SERS signal enhancement than Au and Cu substrate. The result of our simulation is consistent with other model simulation obtained in previous reports [33–35], indicating that the model is feasible. In general, above obtained results indicate that the simulation model and calculation results provide best model for tapered SERS fiber probes applications in the Raman fields.

Table 1
The electric field and enhancement factors of the presented probes in different noble metal substrate and excitation wavelength.

Substrate	λ (nm)	E_{max} (v/m)	EF
Au	532	23.1	2.9×10^5
	633	23.7	3.2×10^5
	785	22.3	2.5×10^5
Ag	532	33.2	1.2×10^6
	633	20.0	1.6×10^5
	785	22.4	2.5×10^5

4. Conclusion

In this study, we have reported a design to tapered optical fiber probes using Ag NPs deposited the fiber tip. The electrical field enhancement and spectrum properties are obtained using 2D-FDTD method. The analysis shows that the electric field enhancement is related to the transmission spectrum. The probe has a stronger electric field intensity compared to the reported modified Au NPs. The influence of the tip radius, conical angle, Ag NPs size and gaps between them on the electric field enhanced has been quantified under typical excitation wavelength of 532, 633 and 785 nm. Moreover, the electric field of the proposed probe is further enhanced from 13.9 to 22.3 times when Au substrate was introduced under the tapered fiber tip. This study can provide theoretical support for tapered fiber probes and assist in preparation of Ag NPs modified fiber tip, and have a reference value for the preparation of tapered fiber optic probes for biosensing applications.

Declarations

Funding: This work was partially supported by the National Natural Science Foundation of China (Grant NO. 61771240 and 61475071) and the Six Talent Peaks Project in Jiangsu Province of China (XYDXX-058).

Conflicts of Interest: The authors declare no conflicts of interest.

Availability of data and material: Data may be obtained from the authors upon reasonable request.

Authors' Contributions: Xiaolei Yu and Zhimin Zhao performed the conceptualization, methodology, editing, and overall supervision. Ciyong Gu performed the model, writing and simulation. Delong Meng contributed to the data analysis.

Ethics approval: Approved.

Consent to participate: Approved.

Consent for publication: Approved.

References

1. Fleischmann MP, Hendra PJ, Mcquillan AJ (1974) Raman Spectra of Pyridine Adsorbed at a Silver Electrode. Chem Phys Lett 26(2):163–166
2. Wang D, Li W, Zhang QR, Liang BQ et al (2021) High-performance tapered fiber surface plasmon resonance sensor based on graphene/Ag/TiO_2 layer. Plasmonics 16(6):2291–2303
3. Ghahramani S, Barvestani J, Meshginqalam B (2021) High-performance Opening-up Dual-core Photonic Crystal Fiber Sensors Based on Surface Plasmon Resonance. Plasmonics 17(1):181–191
4. Andrade GFS, Hayashi JG, Rahman MM, Salcedo WJ, Cordeiro CMB, Brolo AG (2013) Surface-enhanced resonance Raman scattering (SERRS) using Au nanohole arrays on optical fiber tips. Plasmonics 8(2):113–1121
5. Tang Y, Yuan H, Chen J, Xing Q, Su R, Qi W, He Z (2019) Polydopamine-Assisted Fabrication of Stable Silver Nanoparticles on Optical Fiber for Enhanced Plasmonic Sensing. Photonic Sens 10(2):97–104
6. Danny CG, Subrahmanyam A, Sai VVR (2018) Development of plasmonic U-bent plastic optical fiber probes for surface enhanced Raman scattering based biosensing. J Raman Spectrosc 49(10):1607–1616
7. Mamun MAA, Yu F, Stoddart PR (2018) Double Clad Fiber Improves the Performance of a Single-Ended Optical Fiber Sensor. J Lightwave Technol 36(18):3999–4005
8. Manoharan H, Dharanibalaji KC, Sai VVR (2019) Controlled In-Situ Seed-Mediated Growth of Gold and Silver Nanoparticles on an Optical Fiber Platform for Plasmonic Sensing Applications. Plasmonics 15(1):51–60
9. Cao J, Mao Q (2016) Tapered Optical Fiber Probe with a Double-substrate Strategy for Surface-enhanced Raman Scattering Detection. Chem Select 1(8):1784–1788
10. Zhou F, Liu Y, Wang H, Wei Y, Zhang G, Ye H, Chen M, Ling D (2020) Au-nanorod-clusters patterned optical fiber SERS probes fabricated by laser-induced evaporation self-assembly method. Opt Express 28(5):6648–6662
11. Liu C et al (2020) Near-infrared surface plasmon resonance sensor based on photonic crystal fiber with big open rings. Optik 207:164466

12. Yin Z, Geng Y, Xie Q, Hong X, Tan X, Chen Y, Wang L, Wang W, Li X (2016) Photoreduced silver nanoparticles grown on femtosecond laser ablated, D-shaped fiber probe for surface-enhanced Raman scattering. Appl Opt 55(20):5408–5412
13. Xiao G, Yang H (2019) Modeling of Refractive Index Sensing Using Au Aperture Arrays on a Bragg Fiber Facet. Photonic Sens 9(4):337–343
14. Li T, Yu Z, Wang Z, Zhu Y, Zhang J (2021) Optimized Tapered Fiber Decorated by Ag Nanoparticles for Raman Measurement with High Sensitivity. Sens (Basel) 21(7):2300
15. Tian M, Lu P, Schulzgen A, Peyghambarian N, Liu DM (2011) Double-resonance plasmon and polarization effects in a SERS fiber sensor with a grid nanostructure. Opt Commun 284(7):2061–2064
16. Xia M, Guo H, Tang J, Li C, Zhao R, Wang L, Liu W, Yang J, Liu J (2018) Simple, repeatable and low-cost SERS fibre probe for fluorochrome detection. Micro & Nano Letters 13(5):714–719
17. Kumar S, Tokunaga K, Namura K (2020) Experimental Evidence of Twofold Electromagnetic Enhancement Mechanism of Surface-Enhanced Raman Scattering. J Phys Chem C 124(38):21215–21222
18. Savaliya P, Dhawan A (2016) Tapered fiber nanoprobes: plasmonic nanopillars on tapered optical fiber tips for large EM enhancement. Opt Lett 41(19):4582–4585
19. Mahros AM, Tharwat MM, Elrashidi A (2016) Exploring the Impact of Nano-Particles Shape on the Performance of Plasmonic Based Fiber Optics Sensors. Plasmonics 12(3):563–570
20. Wang XM, Li X, Liu WH, Han CY, Wang XL (2021) Gas Sensor Based on Surface Enhanced Raman Scattering. Mater (Basel) 1(4):87–88
21. Morozov YM, Lapchuk AS, Prygun AV, Kryuchyn AA, Dostalek J (2020) Investigation of optical fiber-tip probes for common and ultrafast SERS. New J Phys 22(3):033027
22. Huang Z, Lei X, Liu Y, Wang Z, Wang X, Wang Z, Mao Q, Meng G (2015) Tapered Optical Fiber Probe Assembled with Plasmonic Nanostructures for Surface-Enhanced Raman Scattering Application. ACS Appl Materials&Interfaces 7(31):17247–17254
23. Jin D, Bai Y, Chen H, Liu S, Chen N, Huang J, Huang S, Chen Z (2015) SERS detection of expired tetracycline hydrochloride with an optical fiber nano-probe. Anal Methods 7(4):1307–1312
24. Cao J, Zhao D, Mao Q (2017) A highly reproducible and sensitive fiber SERS probe fabricated by direct synthesis of closely packed AgNPs on the silanized fiber taper. Analyst 142(4):596–602
25. Hutter T, Elliott SR, Mahajan S (2018) Optical fibre-tip probes for SERS: numerical study for design considerations. Opt Express 26(12):15539–15550
26. Xiao C, Chen ZB, Qin MZ, Zhang D, Wu X H (2018) SERS polarization-independent performance of two-dimensional sinusoidal silver grating. Appl Phys Lett 113(17):171604
27. Liu C, Yang L, Liu X, Liu Q, Wang F, Sun T, Chu P (2017) Mid-infrared surface plasmon resonance sensor based on photonic crystal fibers. Opt Express 25(13):14238–14246
28. Johnson PB, Christy RW (1972) Optical Constants of the Noble Metals. Phys Rev B 6(12):4370–4379

29. Zhang Z, Chu F, Guo Z, Fan J, Li G, Cheng W (2019) Design and Optimization of Surface Plasmon Resonance Sensor Based on Polymer-Tipped Optical Fiber. J Lightwave Technol 37(11):2820–2827
30. Xu P, Cai TY, Li ZY (2004) Studies on magnetic photonic band-gap material at microwave frequency. Solid State Commun 130(7):451–454
31. Chen G, Wang Y, Xu J, Pan M (2010) Measuring Ensemble-Averaged Surface-Enhanced Raman Scattering in the Hotspots of Colloidal Nanoparticle Dimers and Trimers. J Am Chem Soc 132(11):3644–3645
32. Lu F, Zhang W, Zhang L, Liu M, Xue T, Huang L, Gao F, Mei T (2019) Nanofocusing of Surface Plasmon Polaritons on Metal-Coated Fiber Tip Under Internal Excitation of Radial Vector Beam. Plasmonics 14(6):1593–1599
33. Baibarac M, Cochet M, Lapkowski M, Mihut L, Lefrant S, Baltog I (1998) SERS spectra of polyaniline thin films deposited on rough Ag, Au and Cu. Polymer film thickness and roughness parameter dependence of SERS spectra. Synth Met 96(1):63–70
34. Roguska A, Kudelski A, Pisarek M, Opara M, Janik-Czachor M (2011) Surface-enhanced Raman scattering (SERS) activity of Ag, Au and Cu nanoclusters on TiO2-nanotubes/Ti substrate. Appl Surf Sci 257(19):8182–8189
35. Tang J, Zhang Q, Zeng C, Man SQ (2013) Preparation of large-area surface-enhanced Raman scattering active Ag and Ag/Au nanocomposite films. Appl Phys A 111(4):1099–1105

Figures

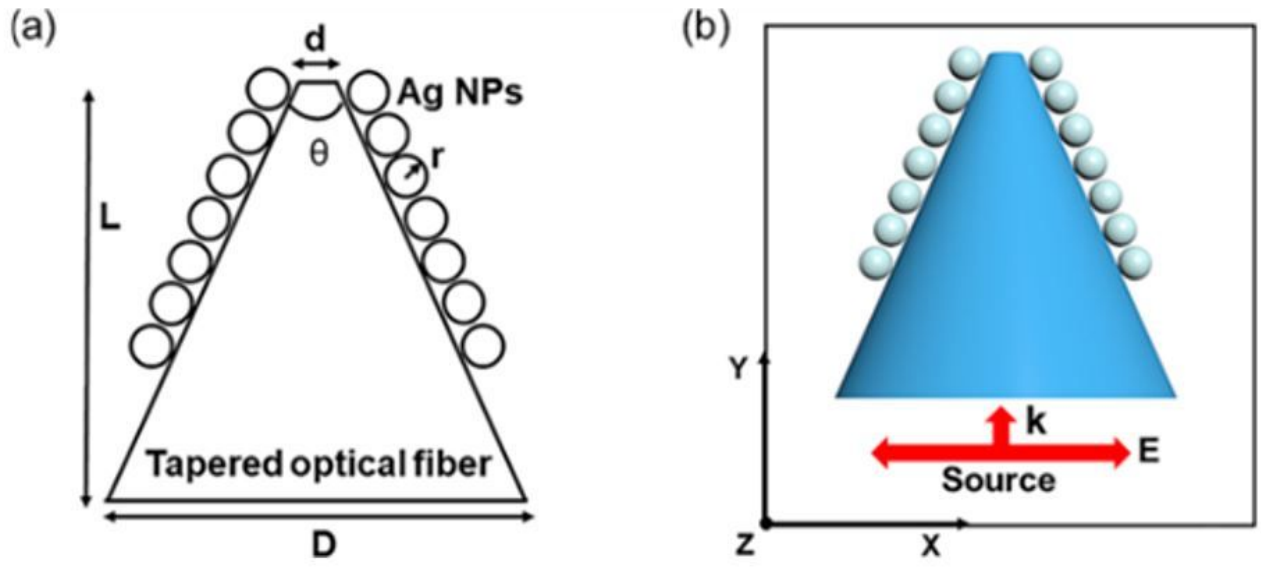

Figure 1

The 2D diagram of the simulation model of tapered optical fiber coated Ag NPs on x-y plane.

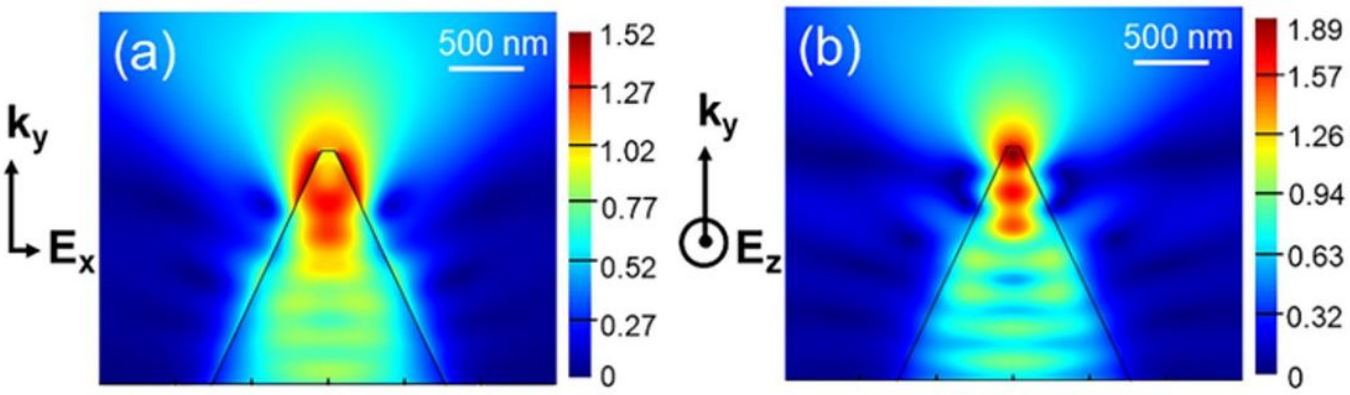

Figure 2

Simulated electric field distribution of the uncoated tapered optical fiber in x-y plane excited by a Gaussian light with a wavelength of 785 nm: (a) p-polarized light;(b) s-polarized light, respectively.

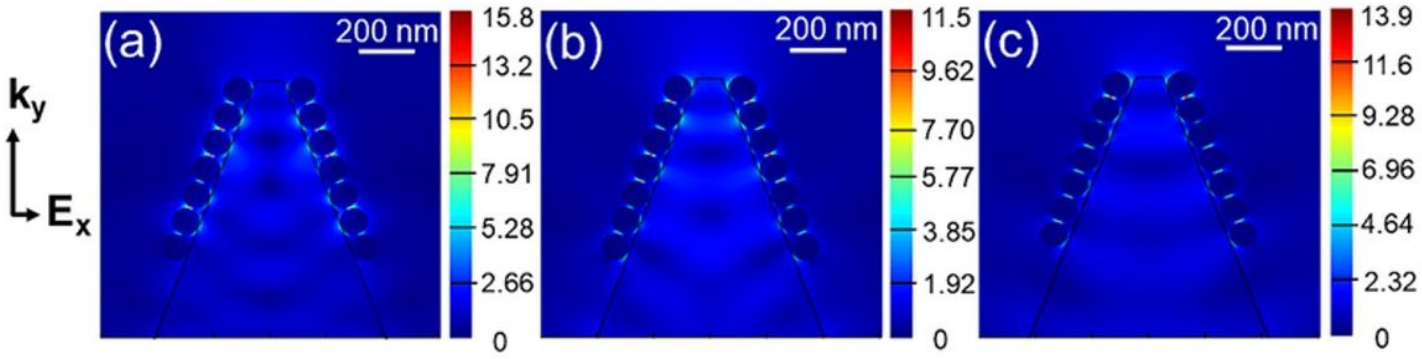

Figure 3

Simulated electric field distribution of tapered optical fiber decorated with Ag NPs in x-y plane excited by a Gaussian p-polarization light with a wavelength of (a) 532 nm; (b) 633 nm; (c) 785 nm, respectively.

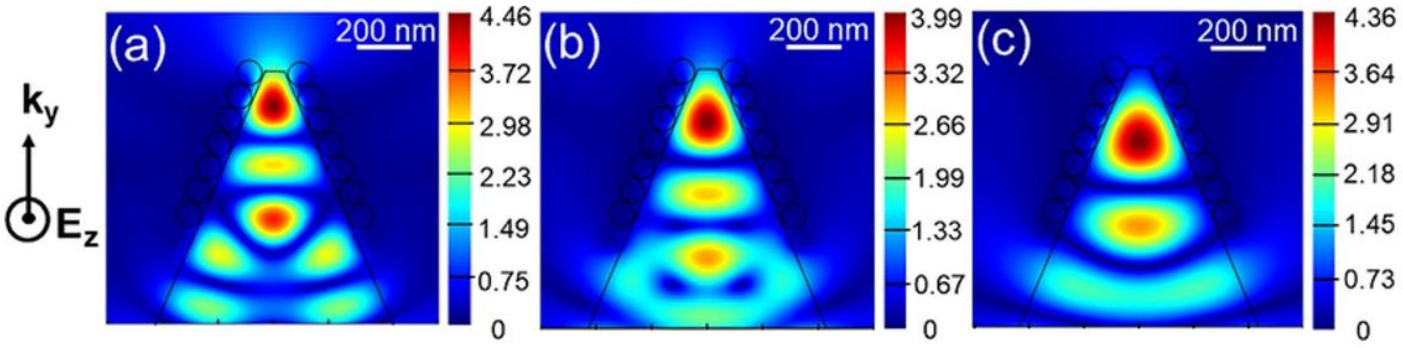

Figure 4

Simulated electric field distribution of the tapered optical fiber decorated with Ag NPs in x-y plane excited by a Gaussian s-polarized light with a wavelength of (a) 532 nm; (b) 633 nm; (c) 785 nm, respectively.

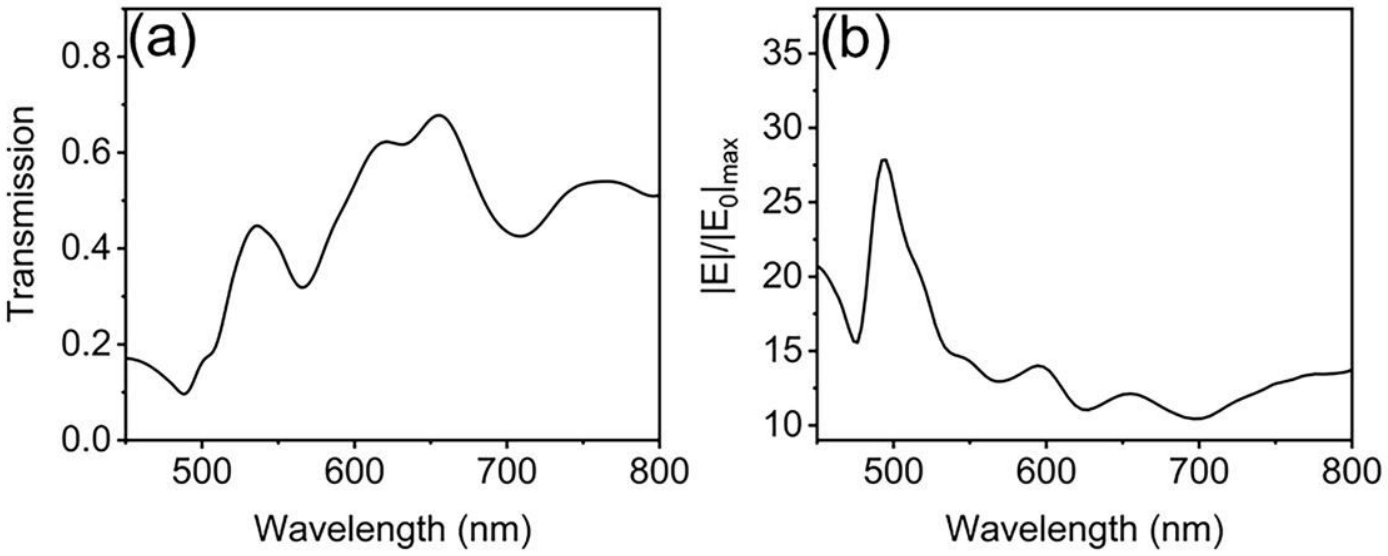

Figure 5

FDTD simulated the transmission spectrums of the tapered optical fiber in p-polarization directions; (b) The maximum electric field of between the Ag NPs in different wavelength.

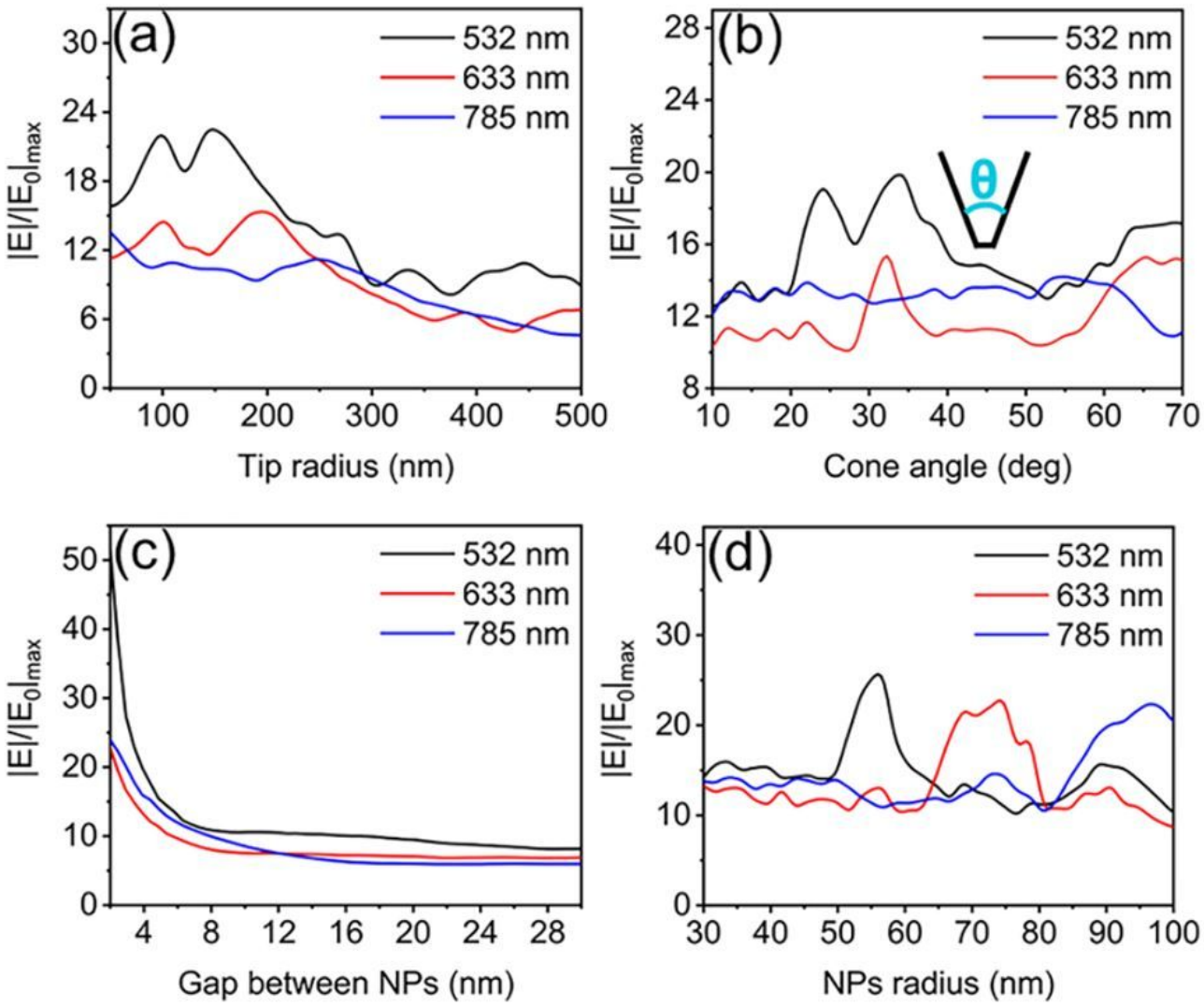

Figure 6

The distribution of maximum electric field enhancement of fiber sensors in x-y plane on different (a) tips radius, (b) cone angles, (c) gap between NPs, and (d) Ag NPs radius under excitation of 532, 633 and 785nm, respectively.

Figure 7

(a) Sketch of the structure of tip-substrate coupling with the distance L of 23 nm; (b) Simulated electric field distributions of the presented probes with an Au substrate in the x-y plane under the excitation wavelength of 785 nm; (c) The relationship between wavelength and electric field of the tip-substrate

coupling and the tip without substrate, measured in x-y plane. (d) The distribution of electric field as the distance L increases, measured in x-y plane.

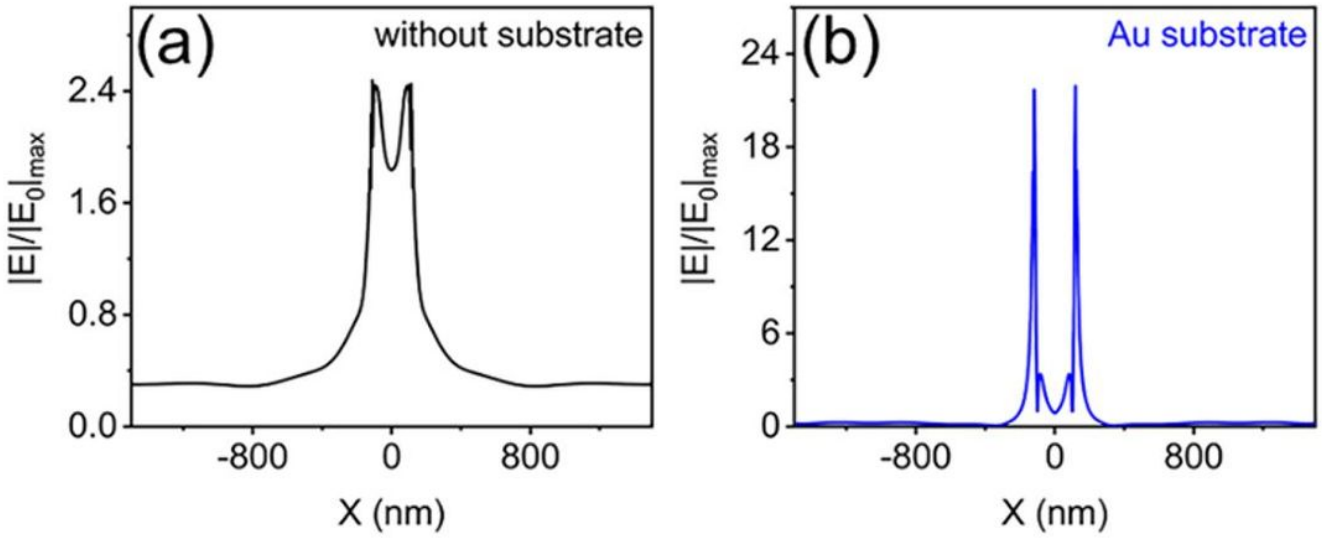

Figure 8

The distribution of electric filed and effective mode area (a) without substrate; (d) with Au substrate.